

# 3D-Environment Measurement System for Large-Scale Structure Manufacturing

Toshiyuki Aoki\*, Kohji Kamejima\*\*

\*Mechanical Engineering Research Laboratory, HITACHI, Ltd  
502 Kandatsu Tsuchiura Ibaraki, Japan, 300  
TEL (0298)32-4111 ext.6421  
FAX (0298)32-2806  
E-mail aoki@merl.hitachi.co.jp

\*\*Department of Industrial Engineering, Osaka Institute of Technology

## Abstract

This paper presents a 3D-environment measurement system for large-scale structure manufacturing.

First, a method and system for generating as-built data are shown. Then a camera calibration method that provides the necessary measurement precision in space is introduced, and the measurement error is analyzed quantitatively. Finally, the position and orientation of an object are measured, and the experimental results are shown to support the theoretical conditions developed here.

## 1. Introduction

For the assembling and maintaining of space structures, teleoperation of working machine [8] will be researched for use in space until the late 1990's. In such situation, the teleoperation system must know the manufacturing environment. However, space structures are made of assembled parts which are manufactured with precision a few millimeters. With such tolerances, errors in the space structures may occur easily, and installation of parts becomes difficult. This kind of problem is solved by measuring the manufacturing environment, storing the measured data in a database, and using this during the design process to ensure that the final design is well adapted to the manufacturing environment. These dynamically changing data are called as-built data and systems that generate as-built data are called manufacturing environment measurement systems.

Measurements are made by using a measuring tape, a light wave surveying machine, or a multilink structure. These measurement methods can give the position of a point, but not the position and orientation of an object. Measurements made by using an image, however, can give the position and orientation of an object [7]. In space, it is necessary to measure objects that can not be touched. We therefore adopt the measurement system using images in the manufacturing environment measurement system.

Many researchers have worked on pattern detection, and we have taken particular note of pattern matching using a pattern field. Pattern detection in random fields by considering the diffusion field [1] has been reported, in which two parameters of the position of an object were estimated. The power and moment in the potential fields were considered, and three parameters of the position and orientation of the object were estimated [2]. Six-degree-of-freedom contour matching through single-eye noisy imagery was reported [6] and six parameters of position

and orientation of the object were estimated. In this paper we adopt this algorithm for automatic pattern matching, and we consider the manufacturing environment measurement system for manufacturing large-scale structures.

First, the method and the system generating the as-built data are shown. Then a camera calibration method that gives the necessary measurement precision in space is introduced, and the measurement error is analyzed quantitatively. Finally, the position and orientation of an object are measured, and the sample experimental data is shown to support the theoretical conditions developed here.

## 2. System Generating As-Built Data

During the manufacture of any particular object, the structure of the object is continually changing. Thus, its design is given concrete shape by the actual work process, for example, by manufacturing, or by carrying and installing structural parts. This changing structure must be continually controlled by using design data.

The precision of as-built data depends on the error of object shapes and on the installation error. The error of object shapes can be controlled during production since the production error is less than a few millimeters. This paper therefore considers the problem of installation error by establishing a measuring method.

The structure must be measured to generate and keep as-built data. This, an interactive system [3] was constructed, using the design data as the prediction data for the position and orientation of the objects (Fig. 2.1).

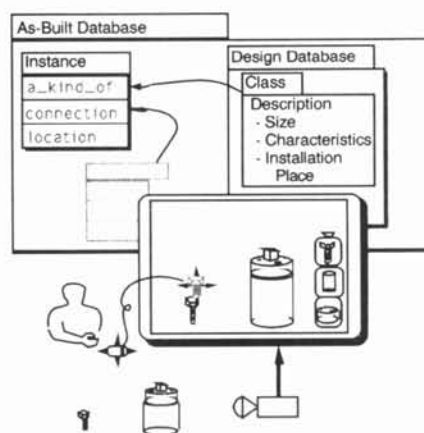


Fig. 2.1. System Generating As-Built Data

In this system, the design data is changed to as-built data by executing the following steps.

- (1) Object images are generated at the site by using CCD cameras, and are then displayed on workstations.
- (2) The position, orientation and shape data of the object is obtained from the design database.
- (3) A wire-frame model is graphically generated from the design data, and is indicated in the same place as the image from the camera.
- (4) An operator roughly matches the wire-frame model to the image model on the display by amending the position and orientation of the object. Also, the wire-frame model is matched to the image model by using the recursive algorithm of six-degree-of-freedom contour matching.
- (5) The position and orientation of the object are saved in the database.

The changing structure can be controlled by iterating the above method.

The object position based on the camera position is determined by matching the wire-frame model to the image model. The measurement precision of the position and orientation of the object is assured by an automatic measuring algorithm [5]. The object position based on the coordinates fixed in the environment must be determined in order to generate the as-built data. Therefore, an appropriate method is to use a surveying machine with a camera, such as that shown in Fig. 2.2. The position and orientation of the object is measured by combining the image with the position and orientation data of the camera.



Fig. 2.2. Surveying Machine with Camera

Although many parts are used in large-scale structure construction, few types of parts are used. Thus, the as-built data structure shown in Fig. 2.3 is appropriate.

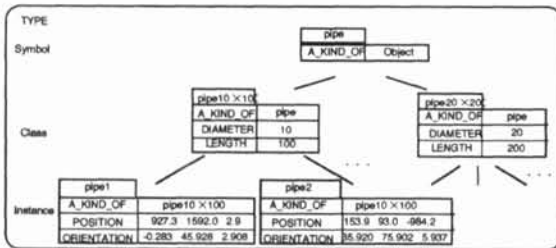


Fig. 2.3. As-Built Data Structure

In Fig. 2.3, each symbol represents a particular type of object. There are various types, such as plates, sleeves, pipes, and so on. The class represents each object shape. For example, the shape of a plate is represented by the lengths of its side and its height, the shape of a sleeve is

represented by its diameter, and the shape of a pipe is represented by its diameter and its length. The instance represents the position and orientation of the object.

### 3. Image Process Identification

#### 3.1 Image Process Model

In the as-built data generation system shown in Fig. 2.1, the image of the structure is generated by using the surveying machine and camera (Fig. 2.2), and the image is displayed on the workstation. The position and orientation of the camera are obtained roughly from the position and orientation of the surveying machine measured by using the surveying machine. The image process is therefore represented by the following equation:

$$\begin{bmatrix} x_m \\ y_m \\ z_m \\ 1 \end{bmatrix} = \begin{bmatrix} 1 & 0 & 0 & 0 \\ 0 & \cos \alpha & -\sin \alpha & 0 \\ 0 & \sin \alpha & \cos \alpha & 0 \\ 0 & 0 & 0 & 1 \end{bmatrix} \begin{bmatrix} \cos \beta & 0 & \sin \beta & 0 \\ 0 & 1 & 0 & 0 \\ -\sin \beta & 0 & \cos \beta & 0 \\ 0 & 0 & 0 & 1 \end{bmatrix} \begin{bmatrix} c_x & 0 & 0 \\ 0 & c_y & 0 \\ 0 & 0 & 1 \\ 0 & 0 & 0 & 1 \end{bmatrix} \begin{bmatrix} e_{mx} \\ e_{my} \\ e_{mz} \\ 1 \end{bmatrix} \begin{bmatrix} x \\ y \\ z \\ 1 \end{bmatrix} \quad (3.1a)$$

$$\begin{bmatrix} x_i \\ y_i \\ 1 \end{bmatrix} = \begin{bmatrix} 1 & 0 & e_x \\ 0 & 1 & e_y \\ 0 & 0 & 1 \end{bmatrix} \begin{bmatrix} c_x & 0 & 0 \\ 0 & c_y & 0 \\ 0 & 0 & 1 \end{bmatrix} \begin{bmatrix} x_m \\ z_m \\ y_m \\ z_m \\ 1 \end{bmatrix} \quad (3.1b)$$

The notations are.

- $x, y, z$ : the object position according to the coordinates fixed by the surveying machine
- $x_m, y_m, z_m$ : the object position according to the camera coordinates
- $x_i, y_i$ : the position of the image model based on the coordinates of the image plane
- $e_{mx}, e_{my}, e_{mz}$ : the camera position according to the surveying machine coordinates
- $\alpha, \beta, \gamma$ : the camera orientation according to the surveying machine
- $c_x, c_y$ : the magnification of the lens, photoelectric conversion, and electric signal conversion
- $e_x, e_y$ : the position of the optical axis according to the coordinates of the image plane

The above parameters depend on the assembly and setup of the surveying machine. Here  $e_{mx}, e_{my}, e_{mz}, \alpha, \beta, \gamma, c_x, c_y, e_x,$  and  $e_y$  are treated as unknown parameters, because the setup can vary according to the actual site conditions.

Since the parameters  $e_{mx}, e_{my}$  and  $e_{mz}$  depend on how well the setup conditions can be duplicated, the variability of parameters  $c_x$  and  $c_y$  depends on the combination of the camera and the workstation, because these parameters depend on the electric displacement of the image. The error of the parameters  $\alpha, \beta, \gamma, e_x,$  and  $e_y$  is small because these

parameters are determined only by the installation error of the camera. In this paper, it is assumed that  $e_x$  and  $e_y$  contain  $\alpha$  and  $\beta$ . The error caused by this assumption is considered in Remark 3.1. The parameter  $\gamma$  is obtained by matching the wire-frame model to the image model.

The image process model is represented by the following equation:

$$\begin{bmatrix} x_m \\ y_m \\ z_m \\ 1 \end{bmatrix} = \begin{bmatrix} \cos \gamma & -\sin \gamma & 0 & e_{mx} \\ \sin \gamma & \cos \gamma & 0 & e_{my} \\ 0 & 0 & 1 & e_{mz} \\ 0 & 0 & 0 & 1 \end{bmatrix} \begin{bmatrix} x \\ y \\ z \\ 1 \end{bmatrix} \quad (3.2a)$$

$$\begin{bmatrix} x_i \\ y_i \\ 1 \end{bmatrix} = \begin{bmatrix} 1 & 0 & e_x \\ 0 & 1 & e_y \\ 0 & 0 & 1 \end{bmatrix} \begin{bmatrix} c_x & 0 & 0 \\ 0 & c_y & 0 \\ 0 & 0 & 1 \end{bmatrix} \begin{bmatrix} \frac{x_m}{z_m} \\ \frac{y_m}{z_m} \\ 1 \end{bmatrix} \quad (3.2b)$$

Here, the unknown parameters are  $\theta = (e_{mx}, e_{my}, e_{mz}, c_x, c_y, e_x, e_y)$ .

Remark 3.1: It can be assumed that the angle between the optical axis and the surveying machine axis is usually small. The parameter  $e_x$  defined in (3.1) is represented by  $e_{ix}$ :

$$e_{ix} = e_x + c_x \tan \alpha \quad (3.3)$$

Thus, the maximum error would be

$$er_\alpha = \left| z_m \left( \frac{\tan(\theta_s/2) \cdot \cos \alpha + \sin \alpha}{-\tan(\theta_s/2) \cdot \sin \alpha + \cos \alpha} - \tan(\theta_s/2) - \tan \alpha \right) \right| \quad (3.4)$$

Here,  $\theta_s$  is the angle of vision, and  $z_m$  is the distance between the camera and the object. The error  $er_\alpha$  is 0.27 mm when  $\theta_s = 20$  degrees,  $z_m = 5,000$  mm and  $\alpha = 0.1$  degrees. This error is acceptable at actual sites. □

### 3.2 Image Process Identification Method

The image process can be simulated by using (3.2). That is, the relative position and orientation between the camera and the object is detected by matching the wire-frame model, which is generated by using (3.2), to the image model. Thus, the parameters represented by (3.2) can be estimated.

The following two principles apply for wire-frame models matched to the image model.

- (1) The image model for which the position and orientation is known is matched to the wire-frame model generated in the same conditions.
- (2) A unique pattern between the wire-frame model and the image model is yielded by changing the position and orientation of the camera (Fig. 3.1).

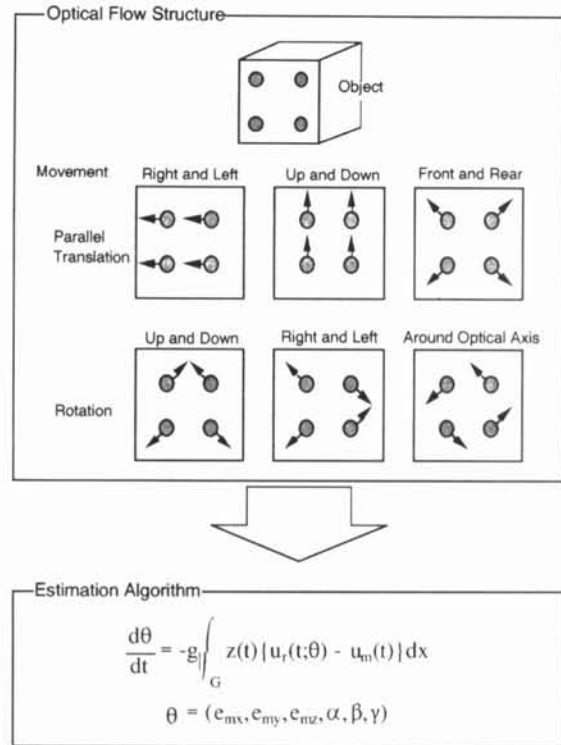


Fig. 3.1. Optical Flow Structure [4]

The unique distortion of the image is yielded corresponding to the camera movement. This distortion is called optical flow. The amount of camera movement is calculated when the optical flow is known. In Fig. 3.1,  $z$  is the optical flow,  $u_m$  and  $u_r$  are the diffusion distributions of the edge pattern and the pattern of the wire-frame model, and  $g$  is gain.

The identification method is based on this principle.

The problem is to obtain the parameters  $\theta = (e_{mx}, e_{my}, e_{mz}, c_x, c_y, e_x, e_y)$  from  $x, y, z, x_i$  and  $y_i$ .

The image process model represented by (3.2) is nonlinear. It is difficult to estimate these parameters because the movements with changes in  $e_{mx}$  and  $e_{my}$  are almost the same as the movements with changes in  $e_x$  and  $e_y$ , respectively. Also,  $e_{mx}$  and  $e_{my}$  cannot be separated from  $e_x$  and  $e_y$ . In this paper, the unknown parameters are estimated by introducing the iterative calculations shown in Fig. 3.2.

For simplicity only the relation between  $x$  and  $z$  is shown in Fig. 3.2. The iterative calculation is executed in the following steps. Objects 1 and 2 are measured by matching the wire-frame model to the image model under the initial condition  $e_x = 0$ , where objects 1 and 2 are set near and far from the camera, respectively. The images of objects 1 and 2 appear at the following positions in the image plane:

$$x_{i1} = c_x \frac{x_1 + e_{mx}}{z_1 + e_{mz}} + e_x \quad (3.5a)$$

$$x_{i2} = c_x \frac{x_2 + e_{mx}}{z_2 + e_{mz}} + e_x \quad (3.5b)$$

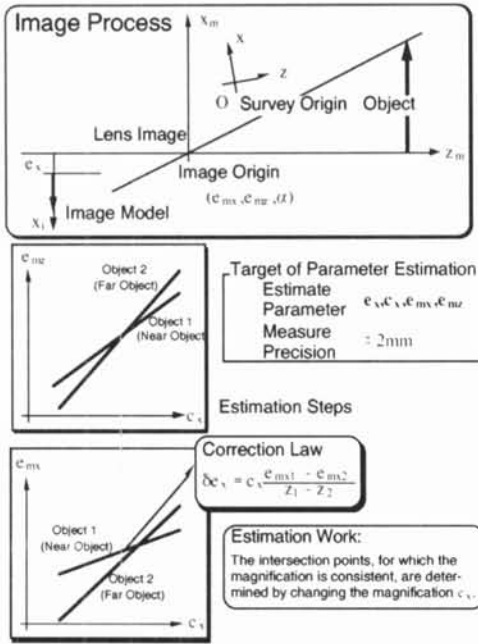


Fig. 3.2. Identification Process

The unknown parameters are estimated by iterating the matching according to the objects far from and near the camera.

The following relations apply between  $c_x$  and  $e_{mx}$ , and between  $c_x$  and  $e_{mz}$ :

$$e_{mx} = \frac{a_1}{c_x} + b_1 \quad (3.6a)$$

$$e_{mz} = a_2 c_x + b_2 \quad (3.6b)$$

Here the parameters  $a_1$ ,  $a_2$ ,  $b_1$ , and  $b_2$  are represented by the following equations:

$$a_1 = - \frac{(z_1 - z_2) [e_x^2 - (x_{i1} - x_{i2})e_x + x_{i1}x_{i2}]}{x_{i1} - x_{i2}} \quad (3.6c)$$

$$b_1 = - \frac{(x_1 - x_2)e_x + x_{i1}x_2 - x_{i2}x_1}{x_{i1} - x_{i2}} \quad (3.6d)$$

$$a_2 = \frac{x_1 - x_2}{x_{i1} - x_{i2}} \quad (3.6e)$$

$$b_2 = \frac{(z_1 - z_2) - x_{i1}z_1 + x_{i2}z_2}{x_{i1} - x_{i2}} \quad (3.6f)$$

Graphs of (3.6a) and (3.6b) can be constructed by changing the magnification and matching the wire-frame model to the image model according to the two objects far from and near the camera. The magnification  $c_x$  corresponding to the two intersection points of the two graphs is consistent if the initial value of  $e_x$  is valid. That is, inconsistency in  $c_x$  is caused by inconsistency in  $e_x$ . When the two intersection points of the two graphs are inconsistent, the parameter  $e_x$  is revised using the following equation:

$$e_x^{n+1} = e_x^n + c_x^n \frac{e_{mx1}(e_x^n) - e_{mx2}(e_x^n)}{z_{m1} - z_{m2}} \quad (3.7)$$

Here  $z_{m1}$  and  $z_{m2}$  represent the distances from the camera to object models 1 and 2 respectively, and  $n$  represents the number of iterations in calculating  $e_x$ . The calculation is iterated by using the revised parameter  $e_x$ , and all parameters are estimated when the calculated parameters converge.

The above steps are summed up as the following:

- (1) The parameter  $e_{mz}$  and  $e_{mx}$  is fixed,  $\gamma$ ,  $\alpha$  and  $c_x$  are obtained by matching the wire-frame model of object 1 to the image model. The same work is executed for object 2. The average of the former  $\gamma$  and the latter  $\gamma$  is calculated and is fixed.
- (2) The parameter  $e_x$  is fixed, and the position and orientation of the camera is measured based on the each magnification by matching the wire-frame model of object 1 to the image model. The parameters  $e_{mx}$  and  $e_{mz}$  corresponding to each magnification  $c_x$  are obtained in this way. From this data the constants in (3.5a) are derived by using the minimum-squares method.
- (3) The same work is executed for object 2, yielding the constants in (3.5b).
- (4) The intersection points of the graphs  $c_x$ - $e_{mx}$  and  $c_x$ - $e_{mz}$  are calculated. This means that (3.6) is valid for objects 1 and 2.
- (5) The calculation is finished when the magnification at the intersection point of graph  $c_x$ - $e_{mx}$  is the same as that of graph  $c_x$ - $e_{mz}$ . When they are not the same, return to (2).

The same algorithm for the  $y$  direction can be attained by using the same method used for the  $x$  direction.

### 3.3 Error Estimate

Here, we quantitatively analyze the error. Image process (3.2) has the following error factors.

- (1) Error of the models of objects 1 and 2 ( $er_1 = 0.5$  mm)

This is the maximum difference in the measured values when ten points are measured by using two surveying machines. This difference depends on the precision of the surveying machine.

- (2) The error caused by the angle measure precision of the surveying machine ( $er_2$ )

$$er_2 = z_m \cdot \tan \delta$$

Here  $\delta$  represents the angle measuring accuracy of the surveying machine.

- (3) The resolution error of the image plane ( $er_3$ )

$$er_3 = \frac{2 \cdot z_m \cdot \tan (\theta_s / 2)}{m \cdot w}$$

Here  $m$  represents the resolution error of the image plane and  $w$  represents the statistical effect during matching.

- (4) The human error during matching ( $er_4$ )
- (5) The approximate error of the camera angle setting ( $er_5$ )

$$er_5 = \left| z_m \left( \frac{\tan(\theta/2) \cdot \cos \lambda + \sin \lambda}{-\tan(\theta/2) \cdot \sin \lambda + \cos \lambda} - \tan(\theta/2) - \tan \lambda \right) \right|$$

Here  $\lambda$  represents the angle between the optical axis of the camera and that of the surveying machine; it is  $\alpha$  or  $\beta$ .

From the above, the equation for predicting error is obtained:

$$er = er_1 + z_m \cdot \tan \delta + \frac{2 \cdot z_m \cdot \tan(\theta/2)}{m \cdot w} + er_4 + \left| z_m \left( \frac{\tan(\theta/2) \cdot \cos \lambda + \sin \lambda}{-\tan(\theta/2) \cdot \sin \lambda + \cos \lambda} - \tan(\theta/2) - \tan \lambda \right) \right| \quad (3.8)$$

The measurement error when using the apparatus shown in Fig. 2.2 is estimated from this equation. For example, when the distance between the camera and the object is 5 m and the object size is 1 m, measurement error is predicted at most to be 2 mm when the resolution of the image plane is 720, the statistical effect of the matching is 2, the angle of vision is 20 degrees, and the angle between the optical axis of the camera and that of the surveying machine is 0.1 degrees.

#### 4. Experimental Results

##### 4.1 Camera Calibration

In Section 3 a measurement precision of  $10^{-4}$  ( $\pm 2$ mm at a distance of 5m between the camera and object) was attained by estimating the camera parameters.

Table 4.1. Camera Parameters

$c_x$	$c_y$	$e_x$	$e_y$
39.745995	31.522924	-0.17317	0.03539
$e_{mx}$	$e_{my}$	$e_{mz}$	
5.67	141.29	-24.885851	

##### 4.2 Determine Precision of Manufacturing Environment Measurement

The position and orientation of the plate is attained using the method shown in Section 2 and the camera parameters listed in Table 4.1.

The measuring precision of the manufacturing environment measurement was also estimated experimentally. A wire-frame model was made using the data measured by the surveying machine. The position and orientation of the plate were measured by using the recursive algorithm for six-degree-of-freedom contour matching. The results are listed in Table 4.6.

Table 4.2. Values Measured by Using Contour Matching

	x	y	z	$\theta_x$	$\theta_y$	$\theta_z$
p11	8097.8	-873.3	-464.3	1.017	0.567	0.231
Difference	1.4	0.2	1.4	1.017	-0.567	0.231

This confirmed that the measurement precision obtained in the error estimate in Section 3 was obtained in the experiment.

#### Conclusions

We have developed a manufacturing environment measurement system that can be used for teleoperation systems. This system obtains the position and orientation of parts by matching a reference pattern to an image model and then storing it in a data base. We then showed an as-built database that has hierarchical structure, the advantage of which is small size.

We derived an image process identification method within the framework of the gradient method, in which it was assumed that the lens magnification contains the camera orientation based on a surveying machine. The error caused by this assumption was estimated.

Then we applied this system to an experimental manufacturing environment. An estimated measurement precision of  $\pm 2$ mm at a distance of 5m between the camera and object was obtained.

#### References

- [1] Kamejima, K., Ogawa, Y. C and Nakano, Y.: A Fast Algorithm for Approximating 2D Diffusion Equation with Application to Pattern Detection in Random Image Fields, Futagami, T., Tzafestas, S.G. and Sunahara, Y. eds., "Distributed Parameter Systems: Modeling and Simulation," Proc. IMACS/IFAC Int. Symp. on Modeling and Simulation of Distributed Parameter Systems, Hiroshima, Japan, 6-9 October, 1987, North Holland, Amsterdam, (1989), pp. 557-564.
- [2] Kamejima, K., Ogawa, Y. C and Nakano, Y.: Perception-Control Architecture in Image Processing for Mobile Robot Navigation System, IECON'84, (1984), pp. 52-57.
- [3] Hamada, T., Kamejima, K. and Takeuchi, I.: Image Based Operation for Human-Robot Interaction, IEEE Control Systems Magazine, 10-6(1990), pp. 24-26.
- [4] Aoki, T. and Kamejima, K.: Six Degree of Freedom Contour Matching through Single Eye Noisy Imagery, 23th ISICIE Symp. on Stochastic Systems, (1991), pp. 97-100.
- [5] Hamada, T., Kamejima, K. and Takeuchi, I.: Dynamic Work Space Model Matching for Interactive Robot Operation, Proc. IEEE Int. Workshop on Industrial Applications of Machine Intelligence and Vision, (1989), pp. 82-87.
- [6] Aoki, T. and Kamejima, K.: A Recursive Optical Flow Approximating Approach to 3D Object Pointing, 24th ISICIE Symp. on Stochastic Systems, (1992.11), pp. 159-162.
- [7] Aoki, T. and Kamejima, K.: Vector Field Matrix Derivation on a Recursive Algorithm of Six Degrees of Freedom Contour Matching, Proceedings of Stochastic Systems Theory and Its Applications, (1993.11), pp. 139-144.
- [8] Kamejima, K., Tsuchiya, M., Kumamoto, K. and Takarada, S.: A Step towards Autonomous Space Robot with an Information-Control Architecture, Pro. i.SAIRAS, (1992).